Application of the Energy Derivative Analysis Method to the *Cis* Monobridged Equilibrium Structures Al_2H_2, Si_2H_2, Ga_2H_2, and Ge_2H_2 and the Comparable Stationary Points of B_2H_2 and C_2H_2

Yukio Yamaguchi,[†] Bradley J. DeLeeuw,[†] Claude A. Richards, Jr.,[†] Henry F. Schaefer III,*[,†] and Gernot Frenking[‡]

Contribution from the Center for Computational Quantum Chemistry, University of Georgia, Athens, Georgia 30602, and Fachbereich Chemie, Institut für Organische Chemie, Philipps-Universität, D-3550 Marburg, Germany

Received April 4, 1994[⊗]

Abstract: An energy derivative analysis method for closed-shell self-consistent field (SCF) wave functions has been applied to the newly (theoretically and/or experimentally) discovered *cis* monobridged compounds Al_2H_2, Si_2H_2, Ga_2H_2, and Ge_2H_2. Monobridged stationary points for the B_2H_2 and C_2H_2 molecules were also considered for comparative purposes. At the stationary points, the first and second derivatives of the orbital, electronic, nuclear, and total energies for SCF wave functions were transformed from the Cartesian to the normal coordinate and to the mass-weighted normal coordinate systems. The energy derivative quantities in terms of the molecular vibrations provide crucial information concerning the structural stability of the monobridged dihydrides of group IIIA and group IVA atoms.

1. Introduction

The global minimum of the ground state of the Si_2H_2 molecule has been found to be a C_{2v} symmetry dibridged (butterfly) form.[1-9] This remarkable structure was first predicted via a theoretical study by Lischka and Köhler in 1983[1] and independently by Binkley[2] a few weeks later. Several years later, a spectroscopic group in France indeed observed this butterfly structure in the laboratory using millimeter- and submillimeter-wave techniques.[10] Further theoretical surveys of the Si_2H_2 potential energy hypersurfaces in our research group led to another exciting discovery in 1990: the existence of a *cis* monobridged structure of the Si_2H_2 molecule.[8,11] After successfully identifying the butterfly structure, the same French group undertook the challenge to synthesize and identify other silicon containing species. In 1992, they reported[12] the spectroscopic observation of this extraordinary monobridged isomer. Here we see a fruitful combined effort of experimental and theoretical work. Remarkable advances in technology and methodology in both experimental measurements and theoretical predictions are without doubt a key point to these successes.

Theoretical consideration has been directed[13-18] subsequently at the potential energy hypersurfaces of other M_2H_2-type molecules, where M denotes a heavy atom of group IIIA or IVA. In these dihydrides, four types of equilibrium structures have been located on the ground state closed-shell singlet surfaces: (1) dibridged structures [nonplanar (C_{2v} symmetry) for Si_2H_2 and Ge_2H_2, planar (D_{2h} symmetry) for Al_2H_2 and Ga_2H_2]; (2) *trans* planar (C_{2h} symmetry) for all four M_2H_2 molecules; (3) *cis* monobridged (C_s symmetry) for all four M_2H_2 molecules; and (4) vinylidene-like structures (C_{2v} symmetry) for all four M_2H_2 molecules. Grev and Schaefer[11] explained the formation of the first three types of compounds as arising from donation of electron density from electron-rich regions (the H atom or the M atom lone pair) to the electron-deficient empty p orbital of an M atom.

Quite recently Chertihin and Andrews have reported[19] matrix-isolated infrared (IR) spectra of AlH_n (n = 1, 2, and 3) and Al_2H_2 species via reactions of pulsed-laser ablated Al atoms with the H_2 molecule. Their detection of planar dibridged (cyclic), *cis* monobridged (asymmetric), and *trans* (symmetric) Al_2H_2 structures is of special interest. They report observation of two absorptions at 1161 (B_{3u}) and 844 cm^{-1} (B_{2u}) for the planar dibridged (cyclic) structure, three absorptions at 1669 (a'), 1127 (a'), and 890 cm^{-1} (a') for the *cis* monobridged

[†] University of Georgia.
[‡] Philipps-Universität.
[⊗] Abstract published in *Advance ACS Abstracts*, November 1, 1994.

(1) Lischka, H.; Köhler, H.-J. *J. Am. Chem. Soc.* **1983**, *105*, 6646.
(2) Binkley, J. S. *J. Am. Chem. Soc.* **1984**, *106*, 603.
(3) Kalcher, J.; Sax, A.; Olbrich, G. *Int. J. Quantum Chem.* **1984**, *25*, 543.
(4) Köhler, H.-J.; Lischka, H. *Chem. Phys. Lett.* **1984**, *112*, 33.
(5) Clabo, D. A., Jr.; Schaefer, H. F. *J. Chem. Phys.* **1986**, *84*, 1664.
(6) Luke, B. T.; Pople, J. A.; Krogh-Jespersen, M.-B.; Apeloig, Y.; Karni, M.; Chandrasekhar, J.; Schleyer, P. von R. *J. Am. Chem. Soc.* **1986**, *108*, 270.
(7) Koseki, S.; Gordon, M. S. *J. Phys. Chem.* **1989**, *93*, 118.
(8) Colegrove, B. T.; Schaefer, H. F. *J. Phys. Chem.* **1990**, *94*, 5593.
(9) Curtiss, L. A.; Raghavachari, K.; Deutsch, P. W.; Pople, J. A. *J. Chem. Phys.* **1991**, *95*, 2433.
(10) Bogey, M.; Bolvin, H.; Demuynck, C.; Destombes, J.-L. *Phys. Rev. Lett.* **1991**, *66*, 413.
(11) Grev, R. S.; Schaefer, H. F. *J. Chem. Phys.* **1992**, *97*, 7990.
(12) Cordonnier, M.; Bogey, M.; Demuynck, C.; Destombes, J.-L. *J. Chem. Phys.* **1992**, *97*, 7984.
(13) Grev, R. S.; DeLeeuw, B. J.; Schaefer, H. F. *Chem. Phys. Lett.* **1990**, *165*, 257.
(14) Palágyi, Z.; Schaefer, H. F.; Kapuy, E. *Chem. Phys. Lett.* **1993**, *203*, 195.
(15) Palágyi, Z.; Schaefer, H. F.; Kapuy, E. *J. Am. Chem. Soc.* **1993**, *115*, 6901.
(16) Palágyi, Z.; Grev, R. S.; Schaefer, H. F. *J. Am. Chem. Soc.* **1993**, *115*, 1936.
(17) Grev, R. S.; DeLeeuw, B. J.; Yamaguchi, Y.; Kim, S.-J.; Schaefer, H. F. In *Structures and Conformations of Non-Rigid Molecules*; Laane, J., Dakkouri, M., van der Veken, B., Oberhammer, H., Eds.; NATO ASI Series C; Kluwer Academic Publishers: Dordrecht, The Netherlands, 1993; Vol. 410, pp 325-342.
(18) Palágyi, Z.; Hu, C.-H.; Meredith, C.; Schaefer, H. F. To be submitted for publication.
(19) Chertihin, G. V.; Andrews, L. *J. Phys. Chem.* **1993**, *97*, 10295.

0002-7863/94/1516-11922$04.50/0

(asymmetric) structure, and a single absorption at 1647 cm^{-1} (B_u) for the *trans* (symmetric) structure. These vibrational frequency assignments were based upon theoretical predictions of the IR intensities; the observed absorptions correspond to IR active modes with the largest intensities.[16]

In a related experimental study Xiao, Hauge, and Margrave have investigated[20] the reactions of gallium with molecular hydrogen and methane via FT-IR matrix isolation spectroscopy. These workers report the observation of two distinct isomers of Ga_2H_2. They give the Ga−H stretching frequency as 1022 cm^{-1} (in Kr matrix) and 1002 cm^{-1} (in Ar matrix) for $Ga_2(b\text{-}H)_2$ with two bridging hydrogens and 1686 cm^{-1} (in Ar matrix) for $Ga_2(t\text{-}H)_2$ with two terminal hydrogens. The Ga−H stretching frequency for the former isomer is consistent with our theoretically predicted[14] values of 1143 cm^{-1} (DZP CISD) and 1139 cm^{-1} (DZP CCSD) for the planar dibridged isomer, and the IR intensity of this B_{3u} mode is determined to be extraordinarily strong. The possibility that the second isomer of Ga_2H_2 might be the monobridged structure was not considered.

In recent studies[21-23] we have reported an extension of the Mulliken−Walsh (M-W)[24,25] diagrams (or rules) to the multidimensional normal coordinate system. Many successful applications of the M-W method to various chemical behaviors simply depend on the fact that responses of the orbital energies are proportional to or equal to responses of the total energy with respect to a certain internal coordinate (in our case normal coordinate). This means that the responses of the one-electron energy and nuclear energy with respect to that coordinate are roughly cancelled out. It has been shown that the first and second derivatives of the orbital, electronic, nuclear, and total self-consistent field (SCF) energies in terms of normal coordinates provide useful information concerning the structures and reactivities of the various molecular systems. This information appears in a mathematically rigorous manner, although it is usually consistent with qualitative bonding models. For each normal coordinate, the orbital energies of certain molecular orbitals (MOs) respond quite sensitively. Those MOs are designated as the vibrationally active molecular orbitals (*va*-MOs). Specifically, the vibrationally active highest occupied and the lowest unoccupied MOs are termed *va*-HOMO and *va*-LUMO, respectively.

In our previous energy derivative analysis studies,[21-23] the normal coordinate system has been predominantly employed to determine the responses of energetic quantities with respect to the molecular vibrations. Namely, the energy derivatives in terms of the Cartesian coordinate ($\mathbf{X}$) system have been transformed into the normal coordinate ($\mathbf{Q}$) systems via the $\mathbf{L_x}$ matrix, where the $\mathbf{L}_x$ matrix connects the two coordinate systems through $\mathbf{X} = \mathbf{L_xQ}$. In the current study, the $\mathbf{L_{xm}}$ matrix which relates the mass-weighted Cartesian coordinate ($\mathbf{X_m}$) and the normal coordinate ($\mathbf{Q}$) systems, $\mathbf{X_m} = \mathbf{L_{xm}Q}$, is also utilized to transform the first- and second-order changes in energetic quantities. The mass-weighted Cartesian coordinate is widely used to pursue the intrinsic reaction coordinate (IRC) originally proposed by Fukui.[26] The IRC, often referred to as the minimum energy path, is the steepest descent path in the mass-weighted Cartesian coordinate system. This coordinate system is also employed in the reaction path Hamiltonian of Miller, Handy, and Adams.[27] There has been extensive development of methods which depend on the availability of analytic higher derivatives of *ab initio* wave functions to determine IRCs. For example, readers may refer to the recent paper by Page, Doubleday, and McIver.[28]

In the present research, we examine the stability of the monobridged structures of six M_2H_2 molecules, namely B_2H_2, C_2H_2, Al_2H_2, Si_2H_2, Ga_2H_2, and Ge_2H_2, using first and second energy derivative analysis methods. Although the B_2H_2 and C_2H_2 potential energy surfaces do not possess planar, monobridged-like equilibrium structures, the analogous stationary points of Hessian index two and one, respectively, are included for comparative purposes. Since the possibility of a monobridged M_2H_2 equilibrium structure had never been proposed prior to Colegrove's 1990 paper,[8] the investigation of the bonding in these systems by the energy derivative is of interest.

2. Theoretical Background

The canonical orbital energies may be commonly determined by diagonalizing the Fock matrix in the MO basis

$$\epsilon_i = F_{ii} = h_{ii} + \sum_{k}^{\text{d.o.}} \{2(ii|kk) - (ik|ik)\} \tag{1}$$

and they may be related to the ionization potential via Koopmans' theorem.[29] In the equation h_{ij} and $(ij|kl)$ are standard one- and two-electron integrals in the MO basis and d.o. denotes doubly occupied orbitals. Using the orbital energies, the electronic energy of a closed-shell SCF wave function may be written as

$$E_{\text{elec}} = \sum_{i}^{\text{d.o.}} (h_{ii} + \epsilon_i) \tag{2}$$

and the total SCF energy as

$$E_{\text{SCF}} = E_{\text{elec}} + E_{\text{nuc}} \tag{3}$$

Energy derivative quantities (for example, the SCF energy) may be transformed from the Cartesian to the normal coordinate system as follows:

first derivative

$$\frac{\partial E_{\text{SCF}}}{\partial \mathbf{Q}} = \frac{\partial E_{\text{SCF}}}{\partial \mathbf{X}} \mathbf{L_x} \tag{4}$$

and second derivative

$$\frac{\partial^2 E_{\text{SCF}}}{\partial \mathbf{Q}^2} = \tilde{\mathbf{L}}_{\mathbf{x}} \frac{\partial^2 E_{\text{SCF}}}{\partial \mathbf{X}^2} \mathbf{L_x} \tag{5}$$

For normal coordinates involving small vibrational amplitudes and/or low frequencies, it is found to be advantageous to use the following mass-weighted energy derivative quantities:

(20) Xiao, Z. L.; Hauge, R. H.; Margrave, J. L. *Inorg. Chem.* **1993**, *32*, 642.
(21) Yamaguchi, Y.; Remington, R. B.; Gaw, J. F.; Schaefer, H. F.; Frenking, G. *J. Chem. Phys.* **1993**, *98*, 8749.
(22) Yamaguchi, Y.; Remington, R. B.; Gaw, J. F.; Schaefer, H. F.; Frenking, G. *Chem. Phys.* **1994**, *180*, 55.
(23) Yamaguchi, Y.; Vacek, G.; Thomas, J. R.; DeLeeuw, B. J.; Schaefer, H. F. *J. Chem. Phys.* **1994**, *100*, 4969.
(24) Mulliken, R. S. *Rev. Mod. Phys.* **1942**, *14*, 204.
(25) Walsh, A. D. *J. Chem. Soc. (London)* **1953**, 2260−2331.
(26) Fukui, K. *J. Phys. Chem.* **1970**, *74*, 4161 (1970). See also: Schaefer, H. F. *Chem. Britain* **1975**, *11*, 227.
(27) Miller, W. H.; Handy, N. C.; Adams, J. E. *J. Chem. Phys.* **1980**, *72*, 99.
(28) Page, M.; Doubleday, C.; McIver, J. W., Jr. *J. Chem. Phys.* **1990**, *93*, 5634.
(29) Koopmans, T. *Physica* **1933**, *1*, 104.

first derivative

$$\mathbf{M}^{1/2}\frac{\partial E_{SCF}}{\partial \mathbf{X}} = \frac{\partial E_{SCF}}{\partial \mathbf{X}}\mathbf{L}_{xm} \tag{6}$$

and second derivative

$$\mathbf{M}\frac{\partial^2 E_{SCF}}{\partial \mathbf{Q}^2} = \tilde{\mathbf{L}}_{xm}\frac{\partial^2 E_{SCF}}{\partial \mathbf{X}^2}\mathbf{L}_{xm} \tag{7}$$

where **M** is the atomic mass matrix.

The energy derivative quantities defined in eqs 4−7 will be employed in order to discuss the structures of the six planar monobridged molecules. In our earlier studies,[21,22] the first derivatives of the canonical orbital energies were determined via analytic derivative techniques. In the present study, the first and second derivatives of energetic quantities (for example, the *i*th orbital energy) were obtained via the finite difference method.

3. Theoretical Procedures

The first and second derivatives of the energy quantities have been determined for the six planar monobridged structures using the triple-ζ plus double polarization (TZ2P) basis set. The triple-ζ (TZ) part of the basis set is Dunning's triple-ζ contraction[30] of Huzinaga's primitive Gaussian sets[31] for B, C, and H. For Al and Si, McLean and Chandler's[32] contractions of Huzinaga's 12s9p primitive Gaussian sets[33] were used. The Ga and Ge TZ basis sets are derived from Dunning's 14s11p5d primitive Gaussian basis sets[34] by loosely contracting to 10s8p2d. The TZ basis set is therefore described as B and C (10s6p/5s3p), Al and Si (12s9p/6s5p), Ga and Ge (14s11p5d/10s8p2d), and H (5s/3s). The TZ2P basis set was constructed by augmenting the TZ basis with two sets of d-like functions on heavy atoms with orbital exponents α_d(B) = 1.40, 0.350; α_d(C) = 1.50, 0.375; α_d(Al) = 0.80, 0.20; α_d(Si) = 1.00, 0.25; α_d(Ga) = 0.216, 0.068; and α_d(Ge) = 0.270, 0.088; and two sets of p functions on hydrogen with orbital exponents α_p(H) = 1.50 and 0.375.

Analytic SCF gradient techniques[35] in conjunction with the Newton−Raphson method were used to locate the stationary point structures for all systems studied. The optimized molecular species were unambiguously characterized using analytic SCF second derivative techniques.[36] The PSI-2 program package[37] has been used in all computational procedures.

4. Results and Discussion

The predicted physical properties of the six planar *cis* monobridged dihydrides, M_2H_2, at the TZ2P SCF level of theory are presented in Table 1. Although the planar monobridged B_2H_2 and C_2H_2 molecules are *not* equilibrium structures, as mentioned above in the Introduction, they are included for comparative purposes.

The Monobridged B_2H_2 Structure: Stationary Point (Hessian Index 2). The predicted geometry at the TZ2P SCF level of theory is depicted in Figure 1. The planar monobridged-like structure for the B_2H_2 molecule is a stationary point with two imaginary vibrational frequencies (Hessian index 2). Following the eigenvector of the 340*i* cm^{-1} out-of-plane bending imaginary frequency leads to the true transition state (Hessian index 1) for the 1,2 hydrogen shift isomerization reaction[18]

$$HB{=}BH \rightarrow :B{-}BH_2 \tag{8}$$

The difference between the two BH* distances is 0.412 Å (1.727 − 1.315), where H* indicates the bridged (migrating) hydrogen atom. Based on an analysis of the SCF eigenvectors, there seems to be no distinct π bonding between the two B atoms.

The energy derivative quantities in terms of the mass-weighted normal and regular normal coordinates, as well as the valence canonical orbital energies, are presented in Table 2. It should be noted that the first derivatives of the energetic quantities with respect to nontotally symmetric normal coordinates vanish due to the total symmetric nature of the energies. The responses for the virtual (unoccupied) orbital energies are omitted from the table because the virtual orbitals at the SCF level of theory are not physically well-defined and they are known to be often too sensitive to the quality of the basis set.[21,38,39]

With respect to the BH stretching (Q_1) mode, the energy of the 4a′ orbital significantly increases. Thus the 4a′ MO is related to the BH bonding orbital, and it is the first-order *va*-MO. In terms of the BH* stretching (Q_2) vibration, the 3a′ orbital energy has a positive slope. For the BB stretching (Q_3) motion, the 3a′ and 5a′ orbital energies show positive gradients. From combined analyses based on the SCF eigenvectors and energy derivatives, the 3a′ and 5a′ MOs may be related to the BB bonding and the BH* bonding orbitals. With the two bending (Q_4 and Q_5) modes, the first-order responses of the orbital energies are relatively small. For all the in-plane vibrations, the 6a′ orbital energy is insensitive. Therefore, the 6a′ MO may be assigned to the lone pair orbital located mainly on the B atom proximate to the H* atom.

When the BH stretching (Q_1) mode is activated, the 3a′ orbital energy shows a negative curvature (second derivative) with a large magnitude, indicating the unstable nature[40] along this stretching coordinate. On the contrary, the curvature of the 4a′ orbital energy is positive, implying the stable (favorable) nature[40] of the BH bond. With respect to the BH* stretching (Q_2) mode, the 3a′ orbital energy shows a negative second derivative and the 5a′ orbital energy has a positive curvature. Thus the 5a′ MO accommodates the migrating H* atom. Upon BB bond elongation (Q_3), the orbital energies of the 3a′, 5a′, and 6a′ MOs have negative curvatures, while the 4a′ orbital energy has a positive second derivative. For this BB stretching motion the responses of the orbital energies are more evident with respect to the mass-weighted normal coordinate than the regular normal coordinate, since the elements of the $\mathbf{L}_{xm}$ matrix have larger absolute values for the heavy atom. For the three stretching (Q_1−Q_3) vibrations, the second derivatives of the electronic energy are negative and those of the nuclear energy are positive.

(30) Dunning, T. H. *J. Chem. Phys.* **1971**, *55*, 716.
(31) Huzinaga, S. *J. Chem. Phys.* **1965**, *42*, 1293.
(32) McLean, A. D.; Chandler, G. S. *J. Chem. Phys.* **1980**, *72*, 5639.
(33) Huzinaga, S. *Approximate Atomic Functions II*; Department of Chemistry Report, University of Alberta, Edmonton, Alberta, Canada, 1971.
(34) Dunning, T. H. *J. Chem. Phys.* **1977**, *66*, 1382.
(35) Pulay, P. *Mol. Phys.* **1969**, *17*, 197.
(36) Osamura, Y.; Yamaguchi, Y.; Saxe, P.; Fox, D. J.; Vincent, M. A.; Schaefer, H. F. *J. Mol. Struct.* **1983**, *103*, 183.
(37) PSI 2.0.8; C. L. Janssen, E. T. Seidl, G. E. Scuseria, T. P. Hamilton, Y. Yamaguchi, R. B. Remington, Y. Xie, G. Vacek, C. D. Sherrill, T. D. Crawford, J. T. Fermann, W. D. Allen, B. R. Brooks, G. B. Fitzgerald, D. J. Fox, J. F. Gaw, N. C. Handy, W. D. Laidig, T. J. Lee, R. M. Pitzer, J. E. Rice, P. Saxe, A. C. Scheiner, and H. F. Schaefer; PSITECH, Inc., Watkinsville, GA, 30677, 1994.
(38) Feller, D.; Davidson, E. R. In *Reviews in Computational Chemistry*; Lipkowitz, K. B., Boyd, D. B., Eds.; VCH Publishers, Inc.: New York, 1990; Vol. 1, pp 1−43.
(39) Davidson, E. R. In *Reviews in Computational Chemistry*, Lipkowitz, K. B., Boyd, D. B., Eds.; VCH Publishers, Inc.: New York, 1990; Vol. 1, pp 373−382.
(40) Yamaguchi, Y.; Alberts, I. L.; Goddard, J. D.; Schaefer, H. F. *Chem. Phys.* **1990**, *147*, 309 and references therein.

Table 1. Theoretical Predictions of the Dipole Moment (μ), Harmonic Vibrational Frequencies (ω), and Infrared Intensities (I) of the Six Planar Monobridged M_2H_2 Molecules Using the TZ2P SCF Level of Theory

M_2H_2	B_2H_2	C_2H_2	Al_2H_2	Si_2H_2	Ga_2H_2	Ge_2H_2
μ (D)	4.716	3.340	0.181	1.344	0.488	0.817
ω_1 (a′) MH stretch (cm^{-1})	2841	3544	1898	2340	1846	2211
ω_2 (a′) MH* stretch	2080	2714	1222	1715	1177	1603
ω_3 (a′) MM stretch	1002	1973	232	666	124	333
ω_4 (a′) MMH bend	810	1019	429	426	397	422
ω_5 (a′) MMH* bend	1091*i*	1011*i*	974	1020	798	890
ω_6 (a″) oop bend	340*i*	621	265	86	273	128*i*
I_1 ($km{\cdot}mol^{-1}$)	55.0	56.8	651.5	68.5	915.2	120.1
I_2	65.2	31.9	450.1	89.8	524.2	129.7
I_3	2.7	7.7	39.5	40.3	9.0	9.1
I_5	26.8	21.0	41.4	13.3	48.6	23.1
I_5	–		718.5	130.2	738.6	104.1
I_6	–	92.6	39.5	52.7	18.9	–

Table 2. The SCF Energy Derivative Quantities for the Planar Monobridged B_2H_2 Stationary Point Using the TZ2P Basis Set[a-g]

	first derivative					second derivative					
normal coord freq	Q_1 2841	Q_2 2080	Q_3 1002	Q_4 810	Q_5 1091*i*	Q_1 2841	Q_2 2080	Q_3 1002	Q_4 810	Q_5 1091*i*	Q_6 340*i*
mass-weighted normal coord											
6a′ (−0.294)	−0.012	−0.015	−0.046	−0.036	−0.056	−0.032	−0.017	−0.261	0.042	−0.099	−0.285
5a′ (−0.421)	−0.068	0.028	0.230	0.017	0.059	−0.043	0.175	−0.106	−0.073	−0.293	0.091
4a′ (−0.648)	0.305	0.063	−0.101	0.019	0.023	0.258	−0.062	0.548	0.516	0.299	0.729
3a′ (−0.777)	−0.017	0.133	0.198	−0.043	−0.070	−0.641	−0.435	−0.385	−0.018	0.114	0.214
normal coordinate											
6a′ (−0.294)	−0.013	−0.011	−0.017	−0.020	−0.040	−0.023	−0.013	−0.020	0.000	−0.068	−0.118
5a′ (−0.421)	−0.029	0.023	0.070	0.022	0.035	−0.017	0.148	−0.011	−0.013	−0.185	0.022
4a′ (−0.648)	0.250	0.054	0.009	−0.003	0.006	0.099	−0.049	0.037	0.254	0.206	0.357
3a′ (−0.777)	0.018	0.120	0.071	−0.005	−0.075	−0.349	−0.356	−0.010	0.013	0.058	0.083
$\partial^n E/\partial Q^n$	1.693	1.996	2.517	−0.386	−0.077	−2.423	−1.460	−0.896	1.588	0.258	1.780
$\partial^n E_{orb}/\partial Q^n$	0.119	0.118	0.034	0.014	−0.120	−0.316	−0.325	0.030	0.162	0.038	0.075
$\partial^n E_{elec}/\partial Q^n$	1.813	2.114	2.551	−0.372	−0.197	−2.739	−1.785	−0.866	1.750	0.295	1.855
$\partial^n E_{nuc}/\partial Q^n$	−1.813	−2.114	−2.551	0.372	0.197	3.830	2.370	1.001	−1.661	−0.456	−1.871
$\partial^n E_{scf}/\partial Q^n$	0.000	0.000	0.000	0.000	0.000	1.091	0.585	0.136	0.089	−0.161	−0.016

[a] With respect to the mass-weighted normal coordinates, first derivatives are in hartree $Å^{-1}$ and second derivatives in hartree $Å^{-2}$. [b] With respect to the normal coordinates, first derivatives are in hartree $Å^{-1}$ $amu^{-1/2}$ and second derivatives in hartree $Å^{-2}$ amu^{-1}. [c] Q_1 = MH stretch (a′); Q_2 = MH* stretch (MH* symmetric stretch) (a′); Q_3 = MM stretch (a′); Q_4 = MMH bend (H*MH bend) (a′); Q_5 = MMH* bend (MH* asymmetric stretch) (a′); and Q_6 = out-of-plane bend (a″). [d] Signs of the normal coordinates are chosen to be positive for increasing bond lengths and bond angles. For the MMH* bending mode, the motion toward the vinylidene-like structure is chosen to be positive. [e] The energy first derivatives with respect to non-totally symmetric modes vanish due to the totally symmetric nature of the energy. [f] Vibrational frequencies are in cm^{-1}. [g] E_h stands for half of the one-electron energy, E_{orb} for the total orbital energy, E_{elec} for the electronic energy, E_{nuc} for the nuclear energy, and E_{scf} for the SCF energy.

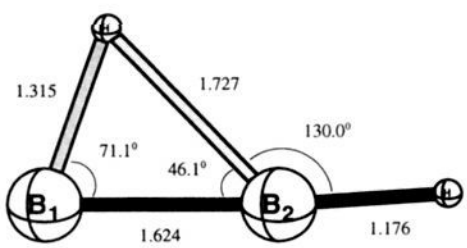

Figure 1. The optimized geometry for the monobridged B_2H_2 (Hessian index 2) stationary point at the TZ2P SCF level of theory. Bond lengths are in Å and bond angles are in deg.

With respect to the BBH bending (Q_4) normal coordinate, the 4a′ orbital energy has a positive curvature. This 4a′ MO is assigned to the BH bonding orbital as mentioned above. For the H* migration (Q_5) mode, the four valence orbital energies have second derivatives with relatively large magnitudes. Thus, all the valence orbitals are second-order *va*-MOs. The orbital energies of the 5a′ and 6a′ MOs have negative curvatures. These negative curvatures are the driving forces for the reaction to proceed to either minimum (reactant or product) in eq 8. Since the 5a′ MO is related to the bonding of the bridged hydrogen to the B atoms, the structural instability of monobridged-like B_2H_2 may be mainly attributed to the *unstable* nature[40] of this orbital along the BBH* bending (Q_5) motion. In terms of the *out-of-plane bending (Q_6) mode, the 3a′, 4a′, and 5a′ orbital* energies have positive second derivatives, while the energy of the 6a′ MO has negative curvature. This negative curvature is a driving force to lead the system to the true isomerization transition state in C_1 symmetry. The existence of a low-lying LUMO (1a″) appears to be responsible for the C_1 symmetry transition state. The 6a′ MO is the second-order *va*-HOMO for the Q_6 vibration, and it coincides with the conventional HOMO.

The energy of the 6a′ MO, which is approximately described as the lone pair orbital on the B atom proximate to H*, has negative curvatures with somewhat large magnitudes for the Q_3, Q_5, and Q_6 modes. The 6a′ MO, therefore, destabilizes the stationary point structure along the BB stretching, BBH* bending, and out-of-plane bending motions. For the three bending (Q_4−Q_6) motions, the electronic energy contributions to the SCF force constants are positive, while the nuclear energy contributions are negative. Since the second derivatives of the total orbital energy and electronic energy are positive, the three bending processes are seen to be electronically stable processes.

The Monobridged C_2H_2 Structure: Transition State (Hessian Index 1). The SCF predicted geometry for planar monobridged-like C_2H_2 is illustrated in Figure 2. This is the transition state structure (Hessian index 1) for the isomerization

Table 3. The SCF Energy Derivative Quantities for the Planar Monobridged C_2H_2 Transition State Using the TZ2P Basis Set[a]

	first derivative					second derivative					
normal coord freq	Q_1 3544	Q_2 2714	Q_3 1973	Q_4 1019	Q_5 1011i	Q_1 3544	Q_2 2714	Q_3 1973	Q_4 1019	Q_5 1011i	Q_6 621
mass-weighted normal coord											
1a″ (−0.435)	−0.082	0.016	0.293	−0.007	−0.013	−0.121	−0.056	−0.685	0.112	0.142	0.374
6a′ (−0.440)	0.048	0.007	−0.120	−0.046	−0.074	−0.001	0.004	−0.156	0.040	~0.014	−0.469
5a′ (−0.570)	−0.075	0.133	0.317	0.067	0.080	−0.070	0.245	−0.302	0.000	~0.484	0.066
4a′ (−0.783)	0.519	0.067	−0.229	0.006	0.046	−0.404	−0.192	0.496	0.859	0.263	0.897
3a′ (−1.105)	−0.109	0.167	0.421	−0.021	−0.079	−0.204	−0.533	0.132	0.124	0.225	0.051
normal coordinate											
1a″ (−0.435)	−0.016	0.021	0.088	0.002	−0.019	−0.030	−0.050	−0.057	0.020	0.061	0.118
6a′ (−0.440)	0.023	0.007	−0.031	−0.020	−0.050	−0.003	0.001	−0.004	0.015	~0.002	−0.160
5a′ (−0.570)	−0.011	0.121	0.097	0.036	0.037	−0.000	0.200	−0.032	0.029	~0.226	0.003
4a′ (−0.783)	0.399	0.049	0.014	−0.001	0.015	−0.324	−0.147	0.024	0.443	0.150	0.458
3a′ (−1.105)	−0.014	0.160	0.134	0.006	−0.082	−0.102	−0.440	0.020	0.017	0.110	−0.008
$\partial^n E_b/\partial Q^n$	1.578	2.870	5.939	0.064	−0.261	−4.365	−3.000	−2.822	2.864	0.717	2.964
$\partial^n E_{orb}/\partial Q^n$	0.370	0.332	0.063	0.029	−0.147	−0.402	−0.441	0.025	0.445	0.123	0.324
$\partial^n E_{elec}/\partial Q^n$	1.948	3.202	6.002	0.094	−0.408	−4.768	−3.441	−2.797	3.308	0.840	3.288
$\partial^n E_{nuc}/\partial Q^n$	−1.948	−3.202	−6.002	−0.094	0.408	6.466	4.436	3.324	−3.168	~0.978	−3.236
$\partial^n E_{scf}/\partial Q^n$	0.000	0.000	0.000	0.000	0.000	1.698	0.995	0.526	0.140	~0.138	0.052

[a] See footnotes $a-g$ in Table 2.

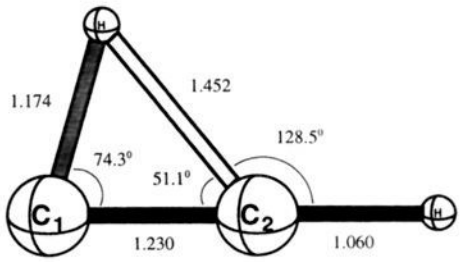

Figure 2. The optimized geometry for the monobridged C_2H_2 (Hessian index 1) stationary point at the TZ2P SCF level of theory. Bond lengths are in Å and bond angles are in deg.

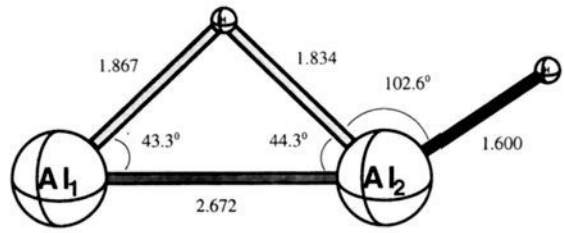

Figure 3. The optimized geometry for monobridged Al_2H_2 at the TZ2P SCF level of theory. Bond lengths are in Å and bond angles are in deg.

(1,2 hydrogen shift) reaction

$$HC{\equiv}CH \rightarrow :C{=}CH_2 \qquad (9)$$

The difference between the two CH* distances is 0.278 Å (1.452 − 1.174), where H* again denotes the bridged (migrating) hydrogen atom. The CC bond shows character intermediate between double and triple bonds. Readers may refer to refs 41−43 for more accurate *ab initio* results for the acetylene−vinylidene system. A detailed energy derivative analysis of this system has also been given elsewhere.[22] The derivatives of the energetic quantities and canonical orbital energies are presented in Table 3. It should be noted that the valence orbital energies are significantly lower for the C_2H_2 system than for the B_2H_2 system. This feature may be attributed to the larger electronegativity[44] of the C atom (2.5) relative to that of the B atom (2.0).

With respect to the reaction coordinate (Q_5), which is approximately described as the CCH* bending mode, the orbital energy of the 5′ MO shows a negative curvature. This negative curvature is a driving force for the reaction to proceed to either minimum (reactant or product) in eq 9. The 5a′ MO describes the BH* and BB bonds in the B_2H_2 system (Table 2) and the CH* and CC bonds in the C_2H_2 system (Table 3), respectively. In these two cases, the BH* and CH* bonds are *not* in the triangular bridged form. The in-plane π-like bonding is more distinct for C_2H_2 than B_2H_2. The structural instability of monobridged-like C_2H_2 may also be attributed to the unstable nature of the 5a′ orbital energy along the Q_5 bending coordinate. The magnitude of the negative curvature of the 5a′ orbital energy with respect to Q_5 is larger for C_2H_2 than for B_2H_2.

For the out-of-plane bending (Q_6, 621 cm^{-1}) mode, the 4a′ and 1a″ orbital energies show large positive curvatures, while the energy of the 6a′ MO has a negative second derivative. The magnitude of the negative curvature of the 6a′ orbital energy is again larger for C_2H_2 than for B_2H_2. The energy of the 1a″ MO, which was unoccupied in the preceding case (B_2H_2), has negative curvatures for the three stretching (Q_1-Q_3) motions and positive curvatures for the three bending (Q_4-Q_6) vibrations. Thus, the 1a″ MO destabilizes the transition state structure along the stretching motions and stabilizes the system along the bending motions. As a result, the SCF force constant of the out-of-plane bending (Q_6) vibration is positive for C_2H_2, in contrast to the negative Q_6 force constant for the B_2H_2 system. Because the second derivatives of the total orbital energy and electronic energy for the reaction coordinate are positive, this isomerization reaction is an electronically stable process.[22]

The Monobridged Al_2H_2 Structure: Equilibrium. The predicted geometry at the TZ2P SCF level of theory is shown in Figure 3. The difference between the two AlH* distances is only 0.033 Å (1.867 − 1.834), where H* indicates the bridged hydrogen atom. Note that in this case the bridged H* atom is slightly closer to the M atom bonded to the terminal H atom. This monobridged structure is a minimum, unlike the cases of B_2H_2 and C_2H_2. The Al−Al bond has single bond character. The energy derivative quantities and valence orbital energies are listed in Table 4. It may be seen that the four valence orbitals of the Al_2H_2 system are higher in energy than those of

(41) Osamura, Y.; Schaefer, H. F.; Gray, S. K.; Miller, W. H. *J. Am. Chem. Soc.* **1981**, *103*, 1904.
(42) Carrington, T.; Hubbard, L. M.; Schaefer, H. F.; Miller, W. H. *J. Chem. Phys.* **1984**, *80*, 4347.
(43) Gallo, M. M.; Hamilton, T. P.; Schaefer, H. F. *J. Am. Chem. Soc.* **1990**, *112*, 8714.

Table 4. The SCF Energy Derivative Quantities for Planar Monobridged Al_2H_2 Using the TZ2P Basis Set[a]

	first derivative					second derivative					
normal coord freq	Q_1 1898	Q_2 1222	Q_3 232	Q_4 429	Q_5 974	Q_1 1898	Q_2 1222	Q_3 232	Q_4 429	Q_5 974	Q_6 265
mass-weighted normal coord											
12a′ (−0.266)	−0.030	−0.025	0.002	0.041	0.028	0.011	0.017	0.134	0.178	0.017	−0.001
11a′ (−0.325)	−0.028	−0.008	0.037	−0.014	−0.069	−0.027	0.057	−0.253	−0.208	−0.051	−0.030
10a′ (−0.470)	0.165	0.051	−0.023	−0.031	0.067	0.063	0.024	0.126	0.085	0.034	0.099
9a′ (−0.590)	0.005	0.152	0.113	0.094	−0.011	−0.199	−0.192	−0.102	−0.078	0.020	0.044
normal coordinate											
12a′ (−0.266)	−0.023	−0.020	−0.008	0.018	0.024	0.005	0.019	−0.003	0.008	0.004	−0.002
11a′ (−0.325)	−0.022	−0.009	0.014	−0.014	−0.062	−0.017	0.039	−0.011	−0.023	−0.032	−0.018
10a′ (−0.470)	0.141	0.041	0.005	−0.004	0.060	0.047	0.021	0.026	0.057	0.039	0.064
9a′ (−0.590)	0.013	0.131	0.006	0.033	−0.017	−0.147	−0.152	0.001	−0.004	0.022	0.040
$\partial^n E_h/\partial Q^n$	3.016	2.892	2.865	2.509	−0.434	−2.894	−0.286	0.114	0.833	−1.477	2.127
$\partial^n E_{orb}/\partial Q^n$	−0.292	0.059	−0.024	−0.020	−0.016	−0.252	−0.386	−0.018	−0.109	0.411	−0.175
$\partial^n E_{elec}/\partial Q^n$	2.724	2.951	2.841	2.489	−0.451	−3.147	−0.671	0.096	0.724	−1.066	1.952
$\partial^n E_{nuc}/\partial Q^n$	−2.724	−2.951	−2.841	−2.489	0.451	3.634	0.873	−0.088	−0.699	1.194	−1.942
$\partial^n E_{scf}/\partial Q^n$	0.000	0.000	0.000	0.000	0.000	0.487	0.202	0.007	0.025	0.128	0.009

[a] See footnotes *a*−*g* in Table 2.

Table 5. The SCF Energy Derivative Quantities for Planar Monobridged Si_2H_2 Using the TZ2P Basis Set[a]

	first derivative					second derivative					
normal coord freq	Q_1 2340	Q_2 1715	Q_3 666	Q_4 426	Q_5 1020	Q_1 2340	Q_2 1715	Q_3 666	Q_4 426	Q_6 1020	Q_6 86
mass-weighted normal coord											
3a″ (−0.283)	−0.029	0.007	0.136	−0.017	−0.010	−0.028	−0.030	−0.212	−0.004	−0.007	−0.025
12a′ (−0.360)	−0.002	−0.029	−0.012	0.035	0.006	0.038	0.039	0.684	−0.005	−0.059	−0.024
11a′ (−0.440)	−0.027	0.071	0.069	−0.066	−0.065	−0.030	0.096	−0.748	−0.086	0.075	−0.021
10a′ (−0.595)	0.228	0.018	−0.104	0.019	0.080	−0.006	−0.006	0.130	0.211	−0.001	0.254
9a′ (−0.776)	0.003	0.149	0.196	−0.016	0.012	−0.228	−0.299	−0.301	0.020	0.040	0.039
normal coordinate											
3a″ (−0.283)	−0.013	0.003	0.025	−0.000	0.000	−0.017	−0.026	−0.007	−0.006	−0.004	−0.017
12a′ (−0.360)	−0.004	−0.023	0.000	0.019	0.005	0.023	0.033	0.032	0.003	−0.045	−0.010
11a′ (−0.440)	−0.013	0.059	0.004	−0.029	−0.054	−0.012	0.083	−0.035	−0.029	0.055	−0.013
10a′ (−0.595)	0.192	0.017	0.005	0.002	0.054	−0.018	−0.010	0.001	0.116	0.013	0.153
9a′ (−0.776)	0.021	0.132	0.041	0.017	0.018	−0.156	−0.246	−0.006	0.009	0.032	0.023
$\partial^n E_h/\partial Q^n$	3.273	4.358	6.974	−0.541	−0.136	−4.215	−2.131	−1.535	1.994	−0.079	2.602
$\partial^n E_{orb}/\partial Q^n$	−0.133	0.027	−0.143	0.054	0.032	−0.222	−0.334	0.000	−0.020	0.289	−0.001
$\partial^n E_{elec}/\partial Q^n$	3.140	4.385	6.831	−0.486	−0.104	−4.437	−2.465	−1.535	1.974	0.210	2.601
$\partial^n E_{nuc}/\partial Q^n$	−3.140	−4.385	−6.831	0.486	0.104	5.177	2.862	1.595	−1.949	−0.069	−2.600
$\partial^n E_{scf}/\partial Q^n$	0.000	0.000	0.000	0.000	0.000	0.740	0.397	0.060	0.025	0.141	0.001

[a] See footnotes *a*−*g* in Table 2.

B_2H_2 (see Table 2) and C_2H_2 (see Table 3) systems, reflecting the smaller electronegativity (1.5)[44] of the Al atom.

With respect to the AlH stretching (Q_1) mode, the energy of the 10a′ orbital increases. Thus the 10a′ MO is assigned to the AlH bonding orbital. In terms of the AlH* symmetric stretching (Q_2) and Al−Al stretching (Q_3) modes, the energy of the 9a′ orbital has positive slopes. From SCF eigenvector and orbital energy derivative analyses, the 9a′ MO may be related to the Al−H*−Al ring (bridged) bonds. The energies of the 11a′ and 12a′ MOs are relatively insensitive in first order to all in-plane vibrational motions. These orbitals are related to the lone-pair-like orbitals on each Al atom, respectively.

For the AlH stretching (Q_1) and AlH* stretching (Q_2) normal coordinates, the 9a′ orbital energy shows negative curvatures, indicating an unstable nature along the two stretching motions. When the AlAl stretching (Q_3) is activated, all the valence orbital energies respond quite sensitively (in the mass-weighted coordinates). The energies of the 9a′ and 11a′ MOs display "instability", while those of the 10a′ and 11a′ MOs are "stable" with respect to the Q_3 coordinate. For the AlH* asymmetric stretching (Q_5) mode, the responses of the orbital energies are somewhat insensitive. Specifically it should be noted that the normal coordinate curvature of the 11a′ orbital energy (−0.032) has a significantly smaller magnitude compared to the corresponding values of the 5a′ orbital energies for B_2H_2 (−0.185) and C_2H_2 (−0.226).

When the AlAlH bending (Q_4, 429 cm^{-1}) motion is activated, the energy of the 11a′ MO has a negative curvature and the 12a′ orbital energy shows a positive second derivative. Thus, this Q_4 mode may be related to the reorganization of the lone-pair-like orbitals on the two Al atoms. In the B_2H_2 and C_2H_2 systems, the MMH bending (Q_4 in Tables 2 and 3) modes were related more closely to the MH bonding orbitals (4a′) than to the lone-pair orbitals. For the out-of-plane bending (Q_6) vibration, all the valence orbital energies have second derivatives with small magnitudes. This feature also differs from the preceding two cases; the curvatures of the 6a′ orbital energy were negative with considerable magnitudes in Tables 2 and 3.

The Monobridged Si_2H_2 Structure: Equilibrium. The TZ2P optimized geometry at the SCF level of theory is illustrated in Figure 4. The monobridged structure of the Si_2H_2 molecule is also a minimum at the TZ2P SCF and correlated levels of theory.[8,11] The difference between the SiH* distances is 0.141 Å (1.759 − 1.618) at the TZ2P SCF level of theory, where H* again denotes the bridged H atom. There is π bonding between the two Si atoms.

The energy derivative quantities and the canonical orbital energies are listed in Table 5. The electronegativity of the Si atom is 1.8,[44] which lies between the corresponding values of the C (2.5) and Al (1.5) atoms. Consequently, the valence

(44) Pauling, L. *Nature of the Chemical Bond*, 3rd ed.; Cornell University Press: Ithaca, NY, 1960.

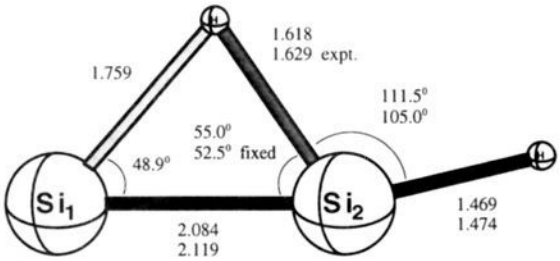

Figure 4. The optimized geometry for monobridged Si_2H_2 at the TZ2P SCF level of theory. Bond lengths are in Å and bond angles are in deg. Experimental values are from ref 12.

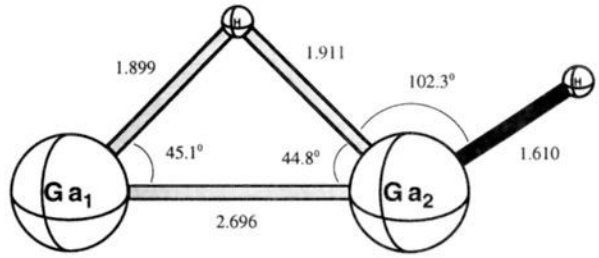

Figure 5. The optimized geometry for monobridged Ga_2H_2 at the TZ2P SCF level of theory. Bond lengths are in Å and bond angles are in deg.

orbital energies for the Si_2H_2 species are higher than those for the C_2H_2 system but lower than those for the Al_2H_2 system. For the SiH stretching (Q_1) mode, the energy of the 10a′ orbital increases. Thus the 10a′ MO is assigned to the SiH bonding orbital. In terms of the SiH* symmetric stretching (Q_2) mode, the energies of the 9a′ and 11a′ MOs have positive slopes. For the SiSi stretching (Q_3) mode, the 9a′, 11a′, and 3a″ orbital energies show positive gradients. From combined analyses of the SCF eigenvectors and orbital energy derivatives, the 9a′ and 11a′ MOs may be related to the triangular Si−H*−Si bridged bonds and the 3a″ MO to the SiSi π bonding orbital. The 11a′ MOs for the Al_2H_2 and Si_2H_2 systems have less distinct in-plane π-like overlap compared to the corresponding 5a′ MOs of the first two molecules.

When the SiH stretching (Q_1) mode is activated, the 9a′ orbital energy shows a negative curvature, indicating unstable nature. For the SiH* symmetric stretching (Q_2) normal coordinate, the energy of the 9a′ MO has a negative second derivative and the 11a′ orbital energy displays positive curvature. In terms of the SiSi stretching (Q_3) mode, all the valence MOs have second derivatives with large magnitudes (in mass-weighted coordinates). The stretching motions are electronically unstable processes, since the second derivatives of the electronic energy are negative.

For the SiSiH bending (Q_4, 426 cm^{-1}) mode, the 10a′ orbital energy shows a stable nature. This feature is similar to that of the Q_4 mode for the C_2H_2 system (see Table 3). With respect to SiH* asymmetric stretching (or SiSiH* bending) Q_5, the 11a′ orbital energy has a positive curvature, in contrast to negative curvatures for the corresponding 5a′ orbital energies of the B_2H_2 and C_2H_2 molecules. In terms of the out-of-plane bending (Q_6, 86 cm^{-1}) vibration, the 10a′ orbital energy has a positive curvature, ensuring the planarity of the monobridged structure. The magnitude of this curvature is substantially larger than the corresponding value of Al_2H_2 (Table 4). The energy of the 3a″ MO, which was unoccupied in the preceding case (Al_2H_2), has negative curvatures for all normal coordinates. This feature is in sharp contrast to the stabilizing nature for the three bending vibrations of the 1a″ MO of C_2H_2 (Table 3) and may be attributed to less efficient hybridization for the second or higher row atoms.[45]

The Monobridged Ga_2H_2 Structure: Equilibrium. The TZ2P SCF optimized geometry is illustrated in Figure 5. The difference between the two GaH* distances is only 0.012 Å (1.911 − 1.899) at this level of theory, where H* indicates the bridged hydrogen atom. The almost isosceles M−H*−M structure is consistent with that of the Al_2H_2 species. There is no apparent π bonding between the two Ga atoms.

The energy derivative quantities and the canonical orbital energies are presented in Table 6. It should be noted that the four valence orbital energies of the Ga_2H_2 system are slightly lower than those of the Al_2H_2 system (in Table 4), because the electronegativity of the Ga atom (1.6) is slightly larger compared to the Al atom (1.5). Relatively large first-order responses of the orbital energies are seen for the 22a′ MO due to the GaH stretching (Q_1) mode, and for the 21a′ MO due to the GaH* stretching (Q_2) and GaGa stretching (Q_3) motions. The 22a′ MO may be related to the GaH bonding and the 21a′ MO to the Ga−H*−Ga bridged bonds. The valence orbital energies are insensitive to the two bending (Q_4 and Q_5) motions, as is usually the case. The energies of the two lone-pair-like orbitals, the 23a′ and 24a′ MOs, have gradients with small magnitudes for all in-plane vibrations.

The second-order responses of the orbital energies for the first four normal coordinates are qualitatively similar to those of the Al_2H_2 species. With respect to the GaH* asymmetric stretching (Q_5) mode, the energies of all the valence orbitals have curvatures with small magnitudes. The curvature of the 23a′ orbital energy with respect to the Q_5 normal coordinate is positive with a small magnitude (0.016) unlike the negative curvature of the 5a′ orbital energy for B_2H_2 (see Table 2). Thus, the bridged H* atom of Ga_2H_2 is more stabilized than that of the B_2H_2 molecule. In terms of the out-of-plane bending (Q_6) mode, the second-order responses of the orbital energies are small in magnitude, as was the case for the Al_2H_2 system (see Table 4). In contrast to the negative curvature of the 6a′ orbital energy of B_2H_2, the 24a′ orbital energy of Ga_2H_2 has a small positive curvature. The planar structure is therefore more stable for the Ga_2H_2 system than the B_2H_2 species.

The Monobridged Ge_2H_2 Structure: Equilibrium (at Correlated Levels). The predicted geometry at the TZ2P SCF level of theory is shown in Figure 6. The planar monobridged structure has one imaginary vibrational frequency. This result is contrary to that for the isovalent Si_2H_2 monobridged species. The normal coordinate corresponding to this SCF imaginary frequency leads to the dibridged (C_{2v} symmetry) global minimum. At correlated levels of theory, however, this structure is found to be a genuine minimum.[15] The out-of-plane bend has a real correlated frequency, and a barrier (with a nonplanar transition state) exists between the planar monobridged and C_{2v} dibridged minima. The difference between the two GeH* distances is 0.144 Å (1.856 − 1.712) at the TZ2P SCF level of theory. This roughly isosceles feature is consistent with that of the Si_2H_2 molecule. The difference in the two GeH* distances is much smaller than those for the B_2H_2 and C_2H_2 monobridged-like structures. There should be π bonding between the two Ge atoms, since the 9a″ orbital is doubly occupied.

(45) Kutzelnigg, W. *Angew. Chem., Int. Ed. Engl.* **1984**, *23*, 272.

Table 6. The SCF Energy Derivative Quantities for Planar Monobridged Ga_2H_2 Using the TZ2P Basis Set[a]

	first derivative					second derivative					
normal coord freq	Q_1 1846	Q_2 1177	Q_3 124	Q_4 397	Q_6 798	Q_1 1846	Q_2 1177	Q_3 124	Q_4 397	Q_5 798	Q_6 273
mass-weighted normal coord											
24a′ (−0.276)	−0.028	−0.024	0.034	0.055	0.040	0.025	0.010	0.155	0.077	−0.011	0.003
23a′ (−0.332)	−0.025	0.002	0.015	−0.038	−0.069	−0.007	0.089	−0.240	−0.096	0.011	−0.029
22a′ (−0.476)	0.142	0.045	−0.041	−0.017	0.054	0.076	−0.017	0.100	0.076	0.008	0.080
21a′ (−0.596)	0.021	0.119	0.131	0.060	−0.022	−0.244	−0.168	−0.217	−0.045	−0.013	0.039
normal coordinate											
24a′ (−0.276)	−0.022	−0.022	−0.005	0.027	0.036	0.019	0.011	−0.002	−0.000	−0.018	0.000
23a′ (−0.332)	−0.023	0.001	0.010	−0.027	−0.064	−0.004	0.071	−0.004	−0.021	0.016	−0.019
22a′ (−0.476)	0.127	0.039	−0.000	0.000	0.051	0.058	−0.014	0.006	0.059	0.014	0.059
21a′ (−0.596)	0.026	0.105	0.009	0.022	−0.027	−0.194	−0.142	−0.000	0.003	−0.011	0.036
$\partial^n E_h/\partial Q^n$	6.955	6.748	11.386	4.940	−1.287	−6.281	−0.892	−0.870	2.966	−1.924	4.805
$\partial^n E_{orb}/\partial Q^n$	−0.609	−0.064	0.007	−0.035	−0.076	−1.560	−1.100	−0.033	−0.336	0.164	−0.438
$\partial^n E_{elec}/\partial Q^n$	6.346	6.684	11.393	4.904	−1.363	−7.841	−1.992	−0.903	2.630	−1.760	4.367
$\partial^n E_{nuc}/\partial Q^n$	−6.346	−6.684	−11.393	−4.904	1.363	8.302	2.179	0.905	−2.609	1.846	−4.357
$\partial^n E_{scf}/\partial Q^n$	0.000	0.000	0.000	0.000	0.000	0.461	0.187	0.002	0.021	0.086	0.010

[a] See footnotes *a*−*g* in Table 2.

Table 7. The SCF Energy Derivative Quantities for Planar Monobridged Ge_2H_2 Using the TZ2P Basis Set.[a]

	first derivative					second derivative					
normal coord freq	Q_1 2211	Q_2 1603	Q_3 333	Q_4 422	Q_5 890	Q_1 2211	Q_2 1603	Q_3 333	Q_4 422	Q_5 890	Q_6 128*i*
mass-weighted normal coord											
9a″ (−0.269)	−0.022	0.006	0.096	0.088	−0.004	−0.028	−0.032	−0.117	−0.088	−0.007	−0.028
24a′ (−0.360)	−0.006	−0.032	−0.004	0.049	0.006	0.047	0.036	0.209	0.387	−0.069	−0.006
23a′ (−0.429)	−0.014	0.076	0.068	−0.014	−0.046	−0.008	0.081	−0.287	−0.414	0.115	−0.021
22a′ (−0.587)	0.189	0.011	−0.086	−0.070	0.055	−0.022	−0.016	0.161	0.116	−0.025	0.177
21a′ (−0.766)	0.011	0.123	0.146	0.143	0.004	−0.204	−0.248	−0.209	−0.203	0.018	0.026
normal coordinate											
9a″ (−0.269)	−0.011	0.002	0.009	0.012	0.000	−0.022	−0.029	−0.005	−0.005	−0.007	−0.020
24a′ (−0.360)	−0.004	−0.028	−0.014	0.023	0.008	0.034	0.033	−0.004	0.013	−0.062	−0.002
23a′ (−0.429)	−0.009	0.067	0.023	−0.025	−0.043	−0.000	0.072	−0.007	−0.027	0.097	−0.013
22a′ (−0.587)	0.167	0.011	−0.002	0.003	0.041	−0.030	−0.018	0.039	0.046	−0.014	0.124
21a′ (−0.766)	0.024	0.111	0.006	0.029	0.007	−0.156	−0.215	0.003	0.001	0.014	0.020
$\partial^n E_h/\partial Q^n$	7.205	9.122	13.567	13.097	−0.076	−8.298	−3.903	0.405	0.790	0.396	5.250
$\partial^n E_{orb}/\partial Q^n$	−0.378	−0.118	−0.078	−0.055	−0.029	−1.266	−1.115	−0.083	−0.092	0.255	−0.075
$\partial^n E_{elec}/\partial Q^n$	6.827	9.003	13.490	13.042	−0.106	−9.564	−5.018	0.322	0.697	0.651	5.175
$\partial^n E_{nuc}/\partial Q^n$	−6.827	−9.003	−13.490	−13.042	0.106	10.225	5.365	−0.307	−0.673	−0.544	−5.177
$\partial^n E_{scf}/\partial Q^n$	0.000	0.000	0.000	0.000	0.000	0.660	0.347	0.015	0.024	0.107	−0.002

[a] See footnotes *a*−*g* in Table 2.

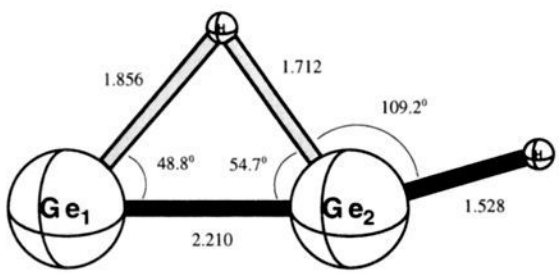

Figure 6. The optimized geometry for monobridged Ge_2H_2 at the TZ2P SCF level of theory. Bond lengths are in Å and bond angles are in deg.

The derivatives of the energetic quantities and the canonical orbital energies are given in Table 7. The valence orbital energies for Ge_2H_2 lie near those of the Si_2H_2 system, reflecting the similar electronegativities[44] of the two atoms [Ge (1.8) and Si (1.8)]. From the first-order positive response of the 22a′ orbital energy to the GeH stretching (Q_1) mode, the 22a′ MO is attributed to the GeH bonding orbital. The 21a′ orbital energy shows prominent responses along the GeH* stretching (Q_2) and GeGe stretching (Q_3) motions. The 21a′ MO is, therefore, related to the Ge−Ge and Ge−H*−Ge triangular (bridged) bonds. The responses of the 9a″ orbital energy (in mass-weighted coordinates) indicate a strong coupling between the Q_3 and Q_4 vibrations. The first derivatives of the 23a′ and 24a′ orbital energies are relatively insensitive to all the in-plane motions. Thus, they may be related to the lone-pair-like orbitals located mainly on the Ge atoms.

With respect to the GeH stretching (Q_1) and GeH* stretching (Q_2) motions, the 21a′ orbital energy shows negative curvatures, as was the case with the corresponding MO of the Si_2H_2 molecule. For the Q_3 and Q_4 vibrations, and 22a′ and 24a′ orbital energies have positive curvatures, while the 21a′, 23a′, and 9a″ orbital energies show negative second derivatives. In terms of the GeH* asymmetric stretching (Q_5) mode, the orbital energy of the 23a′ MO shows a positive curvature, unlike the negative curvature of the corresponding 5a′ orbital energy for C_2H_2 (see Table 3). This positive curvature lends stability to the bridged hydrogen atom. The energies of the three highest occupied orbitals have negative curvatures with small magnitudes for the out-of-plane bending (Q_6) mode. This feature is consistent with the Si_2H_2 system, although the Si_2H_2 molecule has a real out-of-plane bending vibrational frequency at the SCF level of theory, as well as at correlated levels of theory. The energy of the 9a″ MO, which was unoccupied in the preceding system (Ga_2H_2), has negative curvatures for all normal coordinates as was the case for Si_2H_2. The π bonding orbital (9a″), therefore, does not stabilize the system along the vibrational motions.

For the first two stretching (Q_1 and Q_2) motions, the second derivatives of the electronic energy are negative, indicating the

electronically unstable nature of the stretching processes. On the contrary, the four (Q_3–Q_6) vibrational motions have positive electronic energy contributions to the force constants. These molecular vibrations, therefore, are seen to be electronically stable motions.

5. Concluding Remarks

The six planar monobridged dihydrides (M_2H_2), where M is a heavy atom of group IIIA or IVA, have been studied using the energy derivative analysis method. The Si_2H_2 and Al_2H_2 species have been observed in the laboratory.[12,19] Crucial points concerning the structural stability are summarized below.

(i) B_2H_2: The monobridged-like structure has two imaginary vibrational frequencies. The B–H*–B bridge is far from isosceles. The BBH* bending (Q_5) and out-of-plane bending (Q_6) force constants are negative. The curvature of the 5a′ orbital energy with respect to the Q_5 mode and the curvature of the HOMO 6a′ orbital energy with respect to the Q_6 mode are negative with relatively large magnitudes.

(ii) C_2H_2: The monobridged-like structure has one imaginary vibrational frequency. The C–H*–C bridge is far from isosceles. The CCH* bending (Q_5) force constant is negative. The curvature of the 5a′ orbital energy with respect to the Q_5 mode is negative with a substantial magnitude. With respect to the out-of-plane bending (Q_6) mode the curvature of the 6a′ orbital energy is negative and that of the HOMO 1a″ orbital energy is positive.

(iii) Al_2H_2: The monobridged structure is a stable minimum. The Al–H*–Al bridge is *almost* isosceles. The AlH* asymmetric stretching (Q_5) force constant is positive. The curvature of the 11a′ orbital energy with respect to the Q_5 mode is negative with a small magnitude. The curvature of the HOMO 12a′ orbital energy with respect to the Q_6 mode is vanishingly small.

(iv) Si_2H_2: The monobridged structure is a stable minimum. The Si–H*–Si bridge is *near* isosceles. The SiH* asymmetric stretching (Q_5) force constant is positive. The curvature of the 11a′ orbital energy with respect to the Q_5 mode is positive with a small magnitude. The curvatures of the 12a′ and HOMO 3a″ orbital energies with respect to the Q_6 mode are negative with small magnitudes.

(v) Ga_2H_2: The monobridged structure is a stable minimum. The Ga–H*–Ga bridge is *almost* isosceles. The GaH* asymmetric stretching (Q_5) force constant is positive. The curvature of the 23a′ orbital energy with respect to the Q_5 mode is positive with a small magnitude. The curvature of the HOMO 24a′ orbital energy with respect to the Q_6 mode is vanishingly small.

(vi) Ge_2H_2: The monobridged structure is stable at correlated levels of theory and has a single low-magnitude imaginary frequency at the SCF level of theory. The Ge–H*–Ge bridge is *near* isosceles. The GeH* asymmetric stretching (Q_5) force constant is positive. The curvature of the 23a′ orbital energy with respect to the Q_5 mode is positive with a marginal magnitude. The curvatures of the 24a′ and HOMO 9a″ orbital energies with respect to the Q_6 mode are negative with small magnitudes.

The almost and near isosceles structure of monobridged dihydrides containing group IIIA and IVA atoms stabilizes the molecular orbital related to the M–H*–M bridge (11a′ for the third-row M atom and 23a′ for the fourth-row M atom) in terms of the M–H*–M asymmetric stretching vibration. For the C_2H_2 system the additional 1a″ (π bonding) orbital stabilizes the system along the bending vibrations. On the other hand, the π bonding orbitals of Si_2H_2 (3a″) and Ge_2H_2 (9a″) do not have stabilizing effects along any of the normal coordinates.

Acknowledgment. This research was supported by the U.S. National Science Foundation, Grant No. CHE-9216754.